Neutron capture cross sections for nuclei taking part in the main component of s-process

Saumi Dutta[1],* Dipti Chakraborty, G. Gangopadhyay[2], and Abhijit Bhattacharyya[3]
Department of Physics, University of Calcutta,
92, Acharya Prafulla Chandra Road, Kolkata-700009, India

Introduction

About half of the elements heavier than iron are produced by the slow neutron capture process or s-process. The s-process is subdivided into three components namely, weak ($56 < A < 100$), main ($100 < A < 208$), and strong (proposed to describe the abundance peak at ^{208}Pb) components. The nuclei near the vicinity of the $N = 82$ closed shell act as bottlenecks to the main component of s-process reaction flow due to smallness of neutron capture cross sections. The determination of exact nucleosynthesis path for s-process by a network calculation requires the knowledge of the radiative neutron capture cross sections. The (n, γ) crosss sections are also important for s-process branching analysis that can give crucial information about the constraints of astrophysical medium. The reactions in the high temperature stellar environments are thermalized and hence, in general, the cross sections are averaged over the Maxwell-Boltzmann distribution and termed as Maxwellian-averaged cross sections (MACS).

Theory and model calculation

We have calculated the radiative total (n, γ) cross sections in theoretical statistical Hauser-Feshbach formalism with the reaction code TALYS1.6 [1]. The folded potential is constructed by convoluting the target radial matter densities $\rho(r)$ with the standard DDM3Y nucleon-nucleus interaction $v(r)$ [2] as, $V_{fold} = \int v(\mathbf{r} - \mathbf{r}\prime)\rho(\mathbf{r}\prime)d\mathbf{r}\prime$. The matter densities are obtained from relativistic mean field

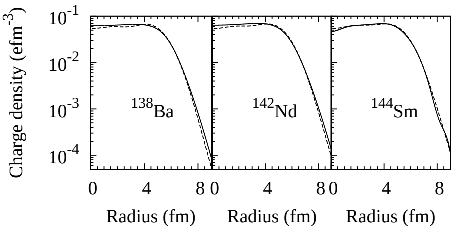

FIG. 1: Charge density in several $N = 82$ nuclei. Solid lines denote the parameterized model values, obtained from fitting the experimental electron scattering data. Dashed lines indicate our results.

(RMF) model using the standard FSU Gold Lagrangian [3]. The final semi-microscopic optical model potential is obtained by taking the imaginary part identical to the real part of the folded potential and later we have multiplied the parts with normalization constants A_r and A_{im} [2] as, $V_{omp} = A_r V_{fold} + jA_{im}V_{fold}$. In this work, we have taken $A_r = A_{im} = 1$.

RMF densities play significant role in the single folding model analysis of nucleon-nucleus potential. Hence, it is reasonable to see the predictability of the RMF Lagrangian density. The point proton densities are convoluted with the standard Gaussian form factor [4] to obtain the charge densities. Further, we have calculated the root-mean-square radius values using these charge densities and compared both density profiles and rms radius values with experiments.

Results

Fig. 1 shows the theoretical charge density profiles compared to the parameterized model values [5, 6], obtained from fitting the elastic electron scattering experiments. In Table I,

*Electronic address: saumidutta89@gmail.com

TABLE I: Root-mean-sqaure charge radius values of some nuclei studied in the present work.

Nucleus	r_c(fm)		Nucleus	r_c(fm)	
	Exp.	Pres.		Exp.	Pres.
^{137}Ba	4.833	4.837	^{138}Ba	4.838	4.843
^{138}La	4.846	4.856	^{139}La	4.855	4.862
^{136}Ce	4.874	4.858	^{138}Ce	4.873	4.869
^{141}Pr	4.892	4.898	^{142}Nd	4.912	4.915
^{143}Nd	4.923	4.927	^{144}Sm	4.944	4.950

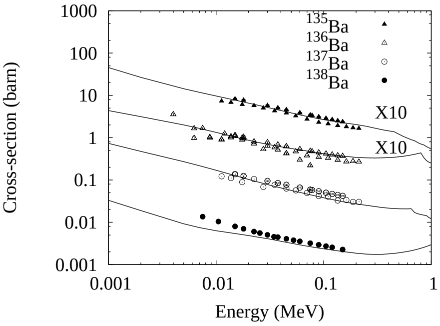

FIG. 2: Comparison of results of the present calculation (solid lines) with experimental data for $^{135-138}$Ba. For convenience, cross-sections for ^{135,136}Ba have been multiplied by a factor of 10.

the root-mean-square charge radius values are compared with the available measurements of Ref. [7]. Fig. 2 shows the (n, γ) cross sections for Ba isotopes from 1 keV to 1 MeV. The experimental values are from Refs. [8–11]. The MACS values at 30 keV are compared with available experimental data and MOST2005 calculations in Table II. The experimental data and MOST values are available in KADoNiS database [12] which is an updated version of the compilation of recommended values by Bao *et al.* [13].

Acknowledgments

Authors thank UGC, DST and AvH Foundation for the financial support.

References

[1] A. J. Koning *et al.*, in *Proc. of the Int. Conf. on Nucl. Data for Science and Technol., April 22-27, 2007, Nice, France*; edited by O. Bersillon *et al.*,(EDP Sciences, Les Ulis, Paris, France, 2008), p. 211 <http://www.talys.eu>
[2] S. Dutta *et al.*, Phys. Rev. C **93**, 024602 (2016).
[3] B. G. Todd-Rutel *et al.*, Phys. Rev. Lett. **95**, 122501 (2005).
[4] A. Bouyssy *et al.*, Phys. Rev. C **36**, 380 (1987).
[5] J. Heisenberg *et al.*, in *Topics in Modern Physics: Tribute to E.U. Condon*, edited by W. E. Brittin and H. Odabasi (Adam Hilger, London, 1970), p 169.
[6] M. A. Moinester *et al.*, Phys. Rev. C **24**, 80 (1981).
[7] I. Angeli, At. Data Nucl. Data Tables **87**, 185 (2004).
[8] F. Voss *et al.*, Phys. Rev. C **50**, 2582 (1994).
[9] F. Voss *et al.*, Phys. Rev. C **52**, 1102 (1995).
[10] H. Beer *et al.*, Astro. J. **474**, 843 (1997).
[11] H. Beer *et al.*, Phys. Rev. C **21**, 534 (1980).
[12] I. Dillmann *et al.*, KADoNiS v0.3 - The third update of the "Karlsruhe Astrophysical Database of Nucleosynthesis in Stars" in *EFNUDAT Fast Neutrons, Proc. of the Sci. Workshop on Neutron Measurements, Theory and Applications* 28 - 30 April 2009, Geel, Belgium; edited by F. -J. Hambsch (Publications Office of the European Union, Luxembourg, 2010) p. 55 ; http://kadonis.org.
[13] Z. Y. Bao *et al.*, At. Data Nucl. Data Tables **76**, 70 (2000).

TABLE II: MACS values at $kT = 30$ keV for a few nuclei near the $N = 82$ shell closure.

Nucleus	MACS(mb)		
	Pres.	Exp.	MOST
$^{136}_{56}$Ba	74.6	61.2±2.0	49.4
$^{137}_{56}$Ba	81.8	76.3±2.4	95.4
$^{138}_{56}$Ba	4.14	4.00±0.20	2.79
$^{138}_{57}$La	417		337
$^{139}_{57}$La	31.0	32.4±3.1	45.9
$^{138}_{58}$Ce	137	179±5	60.5
$^{140}_{58}$Ce	12.7	11.0±0.4	6.71
$^{141}_{59}$Pr	101	111.4±1.4	130
$^{142}_{60}$Nd	54.5	35.0±0.7	22.9
$^{143}_{60}$Nd	362.4	245±3	105
$^{144}_{60}$Nd	82.3	81.3±1.5	37.1
$^{144}_{62}$Sm	91.0	92± 6	38.6